ON THE ELASTICITY OF CYTOSKELETAL NETWORKS

RALPH NOSSAL
Physical Sciences Laboratory, Division of Computer Research and Technology, National Institutes of Health, Bethesda, Maryland 20892

ABSTRACT Models relating to the gelation and elasticity of complex cytoskeletal networks are formulated and investigated. Kinetic equations for reversible elongation of nucleated actin filaments are analyzed when the filaments are acted upon by capping proteins and cross-linking factors. Analytical expressions are obtained that relate the low frequency elastic shear modulus of a network, G, to chain growth kinetics, the number of nucleation sites, monomer concentration, and the amount of capping and cross-linking protein. Elasticity curves that relate G to such factors as the association constant for cross-linking are derived and then used to determine solation–gelation phase contours.

I. INTRODUCTION

A great deal yet remains to be understood about the physical mechanisms governing shape changes and locomotion of biological cells. These and related cellular activities are known to be associated with transient alterations in cytoskeletal structures (1–6), the principal components of which are actin, tubulin, and keratinlike materials that constitute intermediate filaments. These structural proteins react with numerous other proteins and molecular factors, some of which initiate or terminate filament growth, affect polymerization rates, cross-link filaments or form fiber bundles, or cut chains into smaller units (4, 5, 7, 8). Although the biochemical and physiological functions of many such ancillary cytoskeletal proteins are now individually well established, their collective actions need to be further elucidated.

Recent mathematical investigations have shown that several processes, including shape transformations of and material flows within giant ameba (9–12), cellular shape changes correlated with embryotic development (13), and the locomotion of leukocytes and similar cells (14, 15), may depend critically on the rheological state of the cytoplasm. Rheological properties also underlie quantitative in vitro assays for various cytoskeletal constituents that affect network topology (16–18). In the present paper we develop a theory of the elasticity of complex networks, one purpose of which is to improve our intuition about the mechanical behavior of cytoplasmic networks in order to facilitate biophysical modeling of cell locomotion. An additional goal is to derive analytical relationships that can be used to design elasticity assays for cytoplasmic elements.

The work primarily is based on a general molecular theory that relates the shear modulus of a polymer gel to parameters characterizing the chain network responsible for elastic properties (19). The shear modulus, G, links the relative displacement of the parallel faces of an arbitrarily small cubic volume of a material to the forces applied tangentially to those faces, namely, $\sigma = G\gamma$, where σ is the (shear) force per unit area and γ is the shear strain. It should be distinguished from the compressibility modulus, which relates a volumetric change to spatially isotropic pressure forces. A dilute polymer gel has a relatively low shear modulus, but a high compressibility modulus. The natural distortions of cytoplasmic gels therefore would be expected to arise from shear forces rather than compression.

The problem of expressing the macroscopic mechanical properties of a polymer gel in terms of its molecular constituents has not yet been completely solved. Thus, in the following work we necessarily make some compromises, but we believe them to be appropriate for this initial investigation. Basically, we adapt a statistical theory of network elasticity that was developed by assuming that the polymer chains constitute a "phantom network of Gaussian chains." In such theories it is assumed for computational purposes that the bond angles between polymer monomers (or subsets thereof) are randomly distributed, that chain configurations are not affected by the presence of neighboring chains, and that chains can pass freely through each other and even through themselves (19, 20). These assumptions are invoked in many applications of polymer theory and, although the resulting descriptions of network properties frequently are not entirely accurate, they provide meaningful insights into the manner in which such factors as chain length, polymer concentration, cross-link density, and the nature of interchain bonding affect macroscopic elasticity. Our goal here is to provide a minimal theory, but one that contains essential features of the processes being modeled (see section VII).

In particular, we focus on the way that kinetic parameters, such as those influencing strand nucleation, chain growth, and cross-linking, affect elasticity. In this regard, recent experimental evidence affirms the fact that cytoskeletal networks can be elastically rigid even when the

cross-links between network strands are transient, i.e., when the bonds between strands are continuously being broken and reformed (21, 22). The formalism for calculating network elasticity (discussed in section II) is augmented by models for filament nucleation and elongation (sections III and IV), and for interstrand cross-linking (sections III and V). Although results perhaps have more general applicability, here we are concerned implicitly with actin networks. Several assumptions are made that have the effect of simplifying the task of illustrating how the methodology can be employed, but most of those postulates are not critical to the calculations and can be easily modified.

In section V we show how the theory can be used to determine "gelation contours," that is, phase plane projections that describe, e.g., the relationship between cross-link density and the minimum monomer concentration necessary for gelation to occur. We also assess the change in elasticity occurring when various factors such as chain growth kinetics or the number of nucleation sites are varied. In section VI we briefly examine the competitive actions of actin-associated proteins, as epitomized by the simultaneous influence of Ca^{2+} on the formation of bipolar myosin filaments and on the activity of proteins that cause chain fragmentation.

II. NETWORK ELASTICITY

The following analysis is based on a theory of gelation and elasticity of polymer networks that has been developed by Pearson and Graessley (19). In this instance the networks are characterized as consisting of n long primary chains (see Fig. 1), each containing r structural units (e.g., monomers). The chains are divided into strands at junctions, where a junction that unites j units (which requires $j-1$ cross-links) is said to have functionality $2j$. For example, actin-binding protein (ABP), which joins 2 units (23), has a functionality of 4. Because ABP cross-links two chains and consequently unites four strands, it forms a tetrafunctional junction (Fig. 1 *a*). (When actin is polymerized in the presence of high concentrations of ABP, junctions that unite only three strands occasionally are observed [24, 25]; however, tetrafunctional junctions predominate.) Bundling factors generally link a larger number of strands, thus forming junctions of higher functionality. If ω_j is the fraction of all cross-linked units that are found with junctions uniting j units, then $f_\omega \equiv 2\sum_{j=2}^{\infty} j\omega_j$ is the average functionality of the network. The quantity $f_n \equiv 2(\sum_{j=2}^{\infty} \omega_j/j)^{-1}$ is equal to the number-average number of strands leading away from a junction (19).

The fraction of all units that participate directly in cross-links is designated as α. When α exceeds a certain critical value α_c, an infinite three-dimensional network, the "gel cluster," will form. As α increases, a greater proportion of all structural units is connected to the gel cluster. The critical cross-link fraction is given by the derivation of

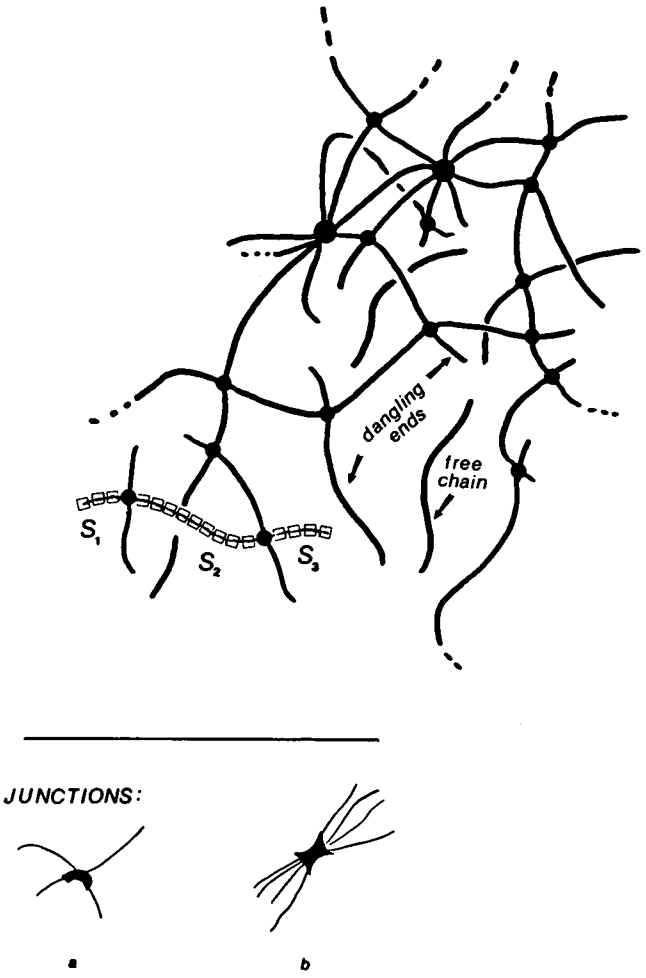

FIGURE 1 Schematic of details of a polymer gel. Lines represent primary chains, consisting of monomers or other elementary units. Junctions (●) divide the primary chains into strands. The polymer lattice comprising the "gel cluster" is that which spans the volume in which it is confined. The sample also might contain free chains or small, isolated clusters that are not connected to the gel cluster. Strands connected to the gel cluster only at one end are called "dangling ends." An "active strand" is connected at both ends to junctions that have at least three paths to the gel cluster. The primary chain highlighted in the lower left is 18 units long ($r = 18$), and is divided by junctions into three strands, two of which (S_1 and S_3) are dangling ends. The junctions shown either have (*a*) 2 units cross-linked, functionality $f = 4$ ("tetrafunctional junctions"), or (*b*) 4 units cross-linked, $f = 8$.

Pearson and Graessley as (19)

$$\alpha_c = \left[\left(\frac{f_\omega}{2} - 1\right)(r-1)\right]^{-1}. \tag{2.1}$$

An expression for the elastic modulus can be obtained (26, 27) by invoking the Scanlon-Case criterion (28, 29), namely, that the shear modulus is proportional to the difference between the number of elastically active stands and the number of elastically active junctions. (A strand is elastically active if both ends are connected to junctions having at least three paths to the gel.) In the case that $\alpha \gg \alpha_c$, it then can be shown that the zero-frequency storage

shear modulus G is linearly dependent upon α, being given as (19)

$$G \approx \left(\frac{\alpha - \alpha_0}{\alpha_0}\right)\frac{\mathcal{N}}{V_0}\Phi k_B T. \tag{2.2}$$

In the above equation, $\mathcal{N}$ is the number of primary strands in the network, V is the volume of the unstressed network, k_B is Boltzmann constant, T is the temperature, Φ is a constant of the order of unity which depends on network topology (26, 27), and the coefficient α_0 is given as (19, 30)

$$\alpha_0 = \left(\frac{1}{1 - \sum_{j=2}^{\infty} \omega_j/j}\right)\frac{1}{r} = \left(\frac{\frac{1}{2}f_n}{\frac{1}{2}f_n - 1}\right)\frac{1}{r}. \tag{2.3}$$

We note that Eqs. 2.1 and 2.3 imply that α_0 is proportional to the critical cross-link fraction α_c according to the relationship

$$\alpha_0 \approx \left[\frac{\sum_{j=2}^{\infty} j\omega_j - 1}{1 - \sum_{j=2}^{\infty} \omega_j/j}\right]\alpha_c = \frac{(\frac{1}{2}f_w - 1)}{(1 - 2f_n^{-1})}\alpha_c. \tag{2.4}$$

For tetrafunctional junctions it follows that $\alpha_0 \approx 2\,\alpha_c$.

The functional dependence of G upon α is shown schematically in Fig. 2. For large values of α/α_c, G varies linearly with α. The extrapolated intercept α_0 is proportional to α_c and thus can be used to study the functional relationships between α_c and experimentally manipulatable quantities. We note, however, that the expression given in Eq. 2.2 pertains to a linear elastic medium, and thus will be applicable only to appropriately small strains. Moreover, Pearson and Graessley's work primarily concerns the statistical problem of calculating the elasticity of phantom networks, that is, relating elastic response to the network topology of a collection of chains that interact only at junction points. The theory, as employed in the present investigation, neglects contributions to elastic properties that arise from chain entanglements. Entropic contributions to elasticity are accounted for, but internal chain energies (e.g., torsional energy associated with chain twisting) are ignored. Also disregarded is the fact that network formation may involve spatial segregation of polymer clusters, which can depend on kinetic determinants such as monomer and cluster diffusion coefficients (31). Such complexities presently are subjects of active research, generally involving much simpler networks than those considered in the present investigation.

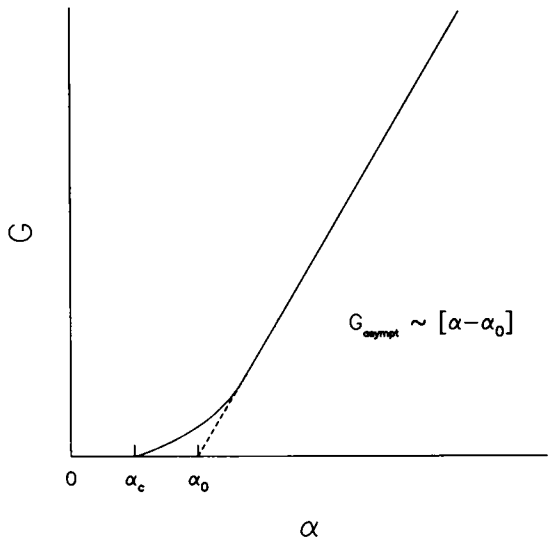

FIGURE 2 The dependence of shear modulus G upon the fraction of units, α, directly incorporated into cross-links. If α is less than a critical value α_c, a spanning network fails to form and the elastic modulus of the polymer lattice is zero. When $\alpha \gg \alpha_c$, the shear modulus is linear with $(\alpha/\alpha_0 - 1)$, where $\alpha_0 \sim \alpha_c$ (cf. Eqs. 2.2 and 2.4).

It is clear from Eq. 2.2 that to analyze cytoskeletal networks one generally needs to determine parameters such as the effective cross-link density and the number and length of primary chains. These will depend on the kinetic coefficients for chain elongation, as well as the binding coefficients involved in cross-link formation. Specific examples illustrating this point are discussed in the following sections.

III. A SPECIAL CASE: FAST, IRREVERSIBLE NUCLEATION

Asymptotic Value of Shear Modulus

We now consider the situation where nucleation of cytoskeletal filaments is rapid compared with chain elongation. Furthermore, we assume that the number of nucleating sites is limiting and that nucleation processes are irreversible. Hence, after a short while the number of chains will equal the number of nucleating sites n_0, and Eq. 2.2 yields

$$G = \left(\frac{\alpha}{\alpha_0} - 1\right)n_0\Phi\frac{k_B T}{V_0}, \tag{3.1}$$

where G now signifies the value of the shear modulus attained after all nucleation reactions have occurred.

By Eq. 2.3 we see that α_0 in this case is given as

$$\alpha_0 \approx \left(\frac{\frac{1}{2}f_n}{\frac{1}{2}f_n - 1}\right)\frac{1}{\langle r\rangle} = \left(\frac{\frac{1}{2}f_n}{\frac{1}{2}f_n - 1}\right)\frac{n_0}{\Delta C}, \tag{3.2}$$

where $\Delta C = n_0\langle r\rangle$ is the total amount of monomer that has been incorporated into polymer chains. The cross-link density α similarly is given as

$$\alpha = \sum_{j=2}^{\infty}(jA_j)/\Delta C, \tag{3.3}$$

where A_j is the number of junctions in the network of functionality $2j$. It is easy to show, from Eq. 3.2, that α_0 is given in terms of A_j as $\alpha_0 = (n_0\Sigma_{j=2}^{\infty} jA_j)/(\Delta C\,\Sigma_{j=2}^{\infty}$

$(j-1)A_j$). Thus, Eq. 3.1 may be rewritten as

$$G = \left[\sum_{j=2}^{\infty}(j-1)A_j - n_o\right]\Phi\frac{k_BT}{V_o}. \quad (3.4)$$

In particular, for a network that is cross-linked only by ABP, which has a functionality of 4, we find from Eqs. 2.4 and 3.4, and the fact that $f_n = f_\omega = 4$,

$$G = (A - n_o)\Phi\frac{k_BT}{V_o}. \quad (3.5)$$

Note that in Eqs. 3.2–3.5 we have implicitly assumed that the distribution of chain lengths is fairly narrow, so that r can be replaced by $\langle r\rangle$. (Pearson and Graessley discuss the general case in an appendix to their paper [19]. It readily can be shown [30] for the case of tetrafunctional junctions that $\alpha_o/(2\,\alpha_c) \approx \langle r\rangle \cdot \langle 1/r\rangle$.)

Crosslinking by Actin-binding Protein

Let us now consider the case appropriate to Eq. 3.5, i.e., cross-linking effected by ABP, in more detail. We first assume the cross-linking reaction as shown in Fig. 3, namely, a molecule of ABP attaches to two contiguous chains to form a junction. S_x designates the concentration of sites where such binding is indeed possible. If all polymerization reactions (yet to be specified) and cross-linking reactions have gone to equilibrium, then, according to the scheme in Fig. 3, the concentration of junctions is given as

$$A = A_oK_xS_x/(1 + K_xS_x), \quad (3.6)$$

where A_o is the total concentration of ABP (including that which has not formed junctions) and K_x is the association constant $K_x = k_B^+/k_B^-$. Of course, the scheme shown in Fig. 3 is a simplification. For example, it subsumes the case of two-step cross-linking where ABP might bind to one strand and later, while still associated, bind to another which might move into appropriate juxtaposition (21, 22). It also ignores the possibility that ABP might also initiate chain growth itself.

S_x depends on the number of overlap points between the polymerized chains, and can be given as

$$S_x \sim (\Delta C)^\beta. \quad (3.7)$$

The correct theoretical value of β is somewhat uncertain. The value obtained in a mean field approximation (20) is $\beta = 2$, but the value $\beta = 9/4$ is obtained from calculations that account for excluded volume (32).

Based on studies that we have performed of several nucleation models for linear chain growth, we infer that the amount of monomer that is incorporated into polymer can be written as

$$\Delta C = (C_o - K^D) \cdot H(n_o, k^+, k_e^+, k_e^-, \ldots), \quad (3.8)$$

where C_o is the total monomer present in the reaction assembly before polymerization occurs, and K^D is the dissociation constant for monomer at the reactive tips of uncapped chains. The function $H(\ldots)$ depends on such variables as the number of nucleation sites, the amount of capping protein, and rate constants associated with chain elongation. Models for chain growth are discussed in the next sections.

IV. A MODEL FOR REVERSIBLE CHAIN ELONGATION

The polymerization reactions are assumed to occur as shown in Fig. 4 (33). An exposed nucleation site, n, reacts with i monomer units ($i = 3$ in Fig. 4) to produce a template (*solid squares*) to which other monomers can join and form primary chains. At each step in the elongation process a capping molecule, e, can bind and thereby terminate chain growth (34, 35). The addition of monomers and caps to elongating chains is considered to be reversible, but template formation here is taken to be an irreversible process. Although not shown in Fig. 4, chain scission (36, 37) can be taken into account (see section VI). Nucleation, which we assume to occur in situ at cell boundaries (38–40), is presumed to be rapid when compared with chain growth and termination (see discussion following Eq. 4.7).

The scheme shown in Fig. 4 is a variant of a simple linear polymerization. Cross-linking reactions are assumed to take place after chain elongation and to be separate processes, occurring by the association of distinct linking molecules with extant chains. Although one might expect that cross-linking (or bundling) and chain growth in reality occur simultaneously, there presently is no evidence that

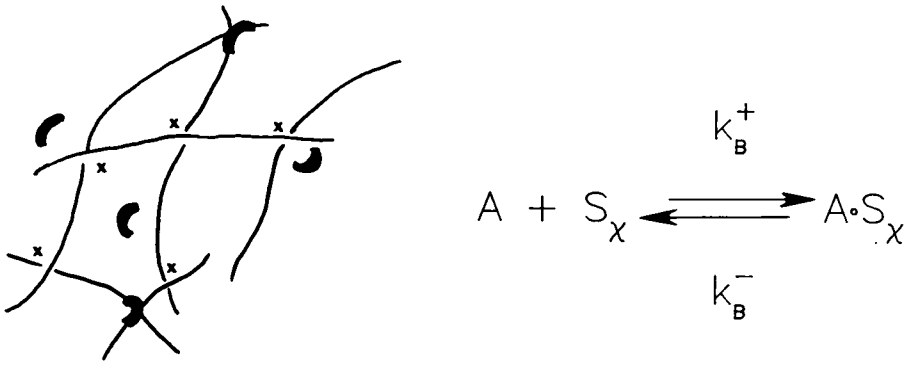

FIGURE 3 Schematic illustration of cross-linking reaction effected by ABP (assumed to form tetrafunctional junctions). A is the concentration of ABP, and S_x is the concentration of possible cross-linking sites (cf. Eq. 3.7).

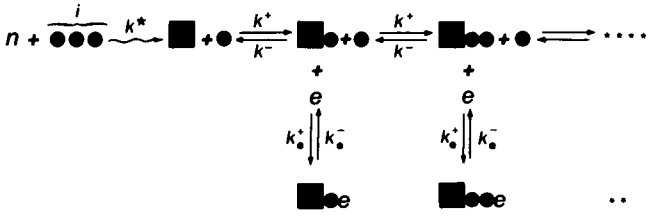

FIGURE 4 Schematic illustration of chain polymerization. A nucleation site n reacts with i monomer units to produce a template (■) to which other monomers can bind and elongate a chain. At each step a capping molecule e can bind and terminate chain growth.

special cross-linking molecules are incorporated into cytoskeletal chains. The time dependence of the development of elastic rigidity may be influenced by temporal relationships between chain growth and cross-linking, but equilibrium properties will not be affected if cross-linking is reversible. (Under certain circumstances, e.g., if the concentration of cross-links is sufficiently high, chain nucleation parameters can be affected by the presence of bundling and cross-linking proteins [7, 8, 24, 25]; such considerations, however, are secondary to our present concerns.)

The depletion of free monomer (e.g., G-actin), which we designate as C_1, is given for this model by the following simple kinetic equation

$$\frac{dC_1}{dt} = -(k^+C_1 - k^-)N, \tag{4.1}$$

where $N(t)$ is the total number of uncapped chains at time t, and k^+ and k^- are the forward and reverse rate constants of polymerization. If we designate $K^D = k^-/k^+$ to be the chain dissociation constant, Eq. 4.1 then has the formal solution

$$C_1(t) = K^D + (C_o - K^D)e^{-k^+\int_0^t N(s)ds}, \tag{4.2}$$

where C_o is defined as $C_o = C_1(0)$.

An equation for chain termination (the conversion of "active" to "capped" chains) is given according to Fig. 4 as

$$\frac{dN}{dt} = -k_e^+ eN + k_e^- \bar{N}, \tag{4.3}$$

where $\bar{N}$ is the total number of capped chains and k_e^+ and k_e^- are rate constants associated with the binding of free capping protein e to the reactive ends of uncapped filaments. Again, because of the assumption of rapid nucleation, the total number of chains is given as $\mathcal{N} = N + \bar{N} = n$, where $n(t) = \int_0^t g_n(s)\,ds$ is the total number of nucleation sites produced up to time t. If we further assume that the generation or potentiation of nucleation sites and capping protein occurs instantaneously (i.e., $g_n(t) = n_o\,\delta^{\text{Dirac}}(t)$ and, similarly, $g_e(t) = e_o\,\delta^{\text{Dirac}}(t)$), Eq. 4.3 may be rewritten as

$$\frac{dN}{dt} = -k_e^+[(e_o - n_o + k_e^-/k_e^+)N + N^2 - (k_e^-/k_e^+)n_o], \tag{4.4a}$$

$$N(0) = n_o.$$

To assess network elasticity, we need to calculate $\Delta C(t) = C_o - C_1(t)$, the amount of monomer incorporated into polymer (cf., Eqs. 3.1 and 3.2). The integral appearing in Eq. 4.2 can be evaluated according to Eq. 4.4a (see Appendix), but the resulting algebraic expressions are rather complicated. For illustration, we consider here the special case that capping protein is in excess, i.e., $\rho \equiv n_o/e_o \ll 1$ (which implies that e is approximately constant). In this instance one finds, instead of Eq. 4.4a,

$$\frac{dN}{dt} \approx -k_e^+[(e_o + k_e^-/k_e^+)N - (k_e^-/k_e^+)n_o] \tag{4.4b}$$

so that, from Eq. 4.2,

$$\Delta C = C_o - C_1(t)$$
$$= (C_o - K^D)\cdot\{1 - \exp[-n_o k^+ f(t)/k_e^+ e_o]\},$$

where $f(t) \equiv (1 + \bar{K}_e^D)^{-2}$

$$\cdot\{1 - \exp[-k_e^+ e_o(1 + \bar{K}_e^D)t] + (1 + \bar{K}_e^D)^{-1}k_e^- t \tag{4.5}$$

and $\bar{K}_e^D \equiv k_e^-/(k_e^+ e_o) \equiv K_e^D/e_o$. ($K_e^D$ is the dissociation constant for capping.) Therefore, if capping is reversible (i.e., $K_e^D \neq 0$), the equilibrium (asymptotic) amount of monomer incorporation is given as

$$\Delta C(t \to \infty) = (C_o - K^D). \tag{4.6}$$

However, if the termination of chains by endcaps is irreversible (i.e., $k_e^- = 0$), the amount of incorporated monomer is

$$\Delta C(t \to \infty) = (C_o - K^D)(1 - e^{-n_o k^+/k_e^+ e_o}). \tag{4.7}$$

In Fig. 5 we show analogous time dependences of $\Delta C(t)$.

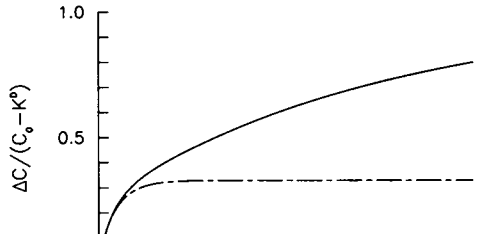

FIGURE 5 The amount of monomer incorporated into polymer chains for the model shown in Fig. 4, assuming that $n_o/e_o \ll 1$. Curves are obtained according to Eq. 4.5 and plotted as $\Delta C(t)/(C_o - K^D)$ vs. the reduced time $\tau = k_e^+ e_o t$. The solid curve pertains to reversible cap formation ($K_e^D \neq 0$) and approaches the value $\Delta C/(C_o - K^D) = 1$, asymptotically. The broken curve corresponds to the case where cap formation is irreversible. The specific values of kinetic constants used in the computations, chosen for illustrative purposes, are $K_e^D = 1.2$, $(n_o k^+)/(k_e^+ e_o) = 0.4$ (cf. Eqs. 4.5–4.7).

When monomeric G-actin polymerizes into filaments, cooperative nucleation usually is the rate-limiting step unless extraneous factors are present (41). By asserting that nucleation is rapid compared with chain elongation, we assume here that polymerization occurs when membrane-bound nucleation sites or F-actin seeds are exposed by an appropriate physiological process. Variations of this kinetic scheme might relate, also, to the growth of actin filaments on the surfaces of polystyrene latex beads (42). A slightly modified model can be used to show that when nucleation sites are generated over an appreciable length of time rather than instantaneously, the amount of monomer incorporated into the chains decreases (if chain elongation and capping reactions are irreversible), there being a concomitant decrease in the modulus.

Other kinetic processes that have been devised to explain in vitro data (e.g., "treadmilling" [43] or ATP capping [44, 45]) probably can be adapted in accordance with the analysis given in the present paper. One also might wish to investigate the consequences of allowing polymerization rates to vary with chain length (41). However, the model given in Fig. 4 allows us to obtain analytical expressions that readily provide insight into the complex ways that the determinants of network polymerization affect elastic properties.

V. DEPENDENCE OF SHEAR MODULUS ON NETWORK PARAMETERS

Preexisting Chains

Eqs. 3.4 and 3.5 are deceptively simple, as they obscure the complex relationships between the number of effective cross-links, A, and the determinants of network topology. The analysis provided in the previous section indicates that the number of potentially effective cross-link sites S_x (Eq. 3.6) critically depends on C_o, n_o, K^D, e_o, K_e^D, and other factors that influence chain growth. If, however, preexisting chains are employed (i.e., the number and lengths of the primary chains are fixed), cross-linking can be studied by conceptually simple elasticity assays. Consider, for example, an assay for ABP (17). If the shear modulus G is measured as a function of the amount of ABP that is added to the reaction mixture, results similar to those shown schematically in Fig. 6 are expected. The slope and intercept of the line drawn through the data points can be interpreted according to Eqs. 3.5 and 3.6 as

$$(\Phi k_B T/V_o)^{-1} \frac{\partial G}{\partial A_o} = K_x S_x (1 + K_x S_x)^{-1} \qquad (5.1)$$

and

$$A_o^* = n_o[(K_x S_x)^{-1} + 1]. \qquad (5.2)$$

Eqs. 5.2 and 3.7 can be used to infer various parametric relationships pertaining to gelation. For example, if conditions are such that $K_x \cdot S_x \ll 1$, it follows that the phase plane for gelation appears as given in Fig. 7. Gelation occurs only if $A > A_o^*(C_o)$, implying that the boundary between the sol and gel phases is defined by the line $A \approx n_o/K_x \cdot S_x \sim (C_o - K^D)^{-\beta}$. Similarly, if the amount of ABP is held constant, solation can be achieved by varying conditions until K_x is reduced to a value such that $K_x < K_x^*$, where K_x^* is given as $K_x^* = [S_x \cdot (A_o/n_o - 1)]^{-1}$. We note from Fig. 8 that, for any given value of A_o/n_o, small variations in K_x can result in dramatic changes in G.

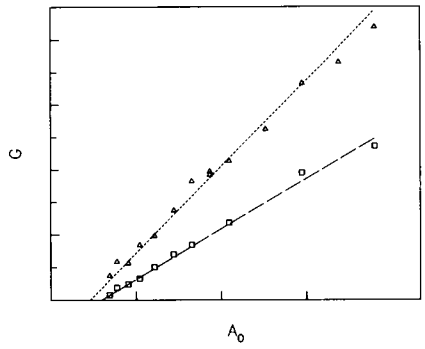

FIGURE 6 Hypothetical results of measurements of shear modulus as amount of cross-linking protein is varied. Data points given by triangles correspond to the situation where the monomer concentration exceeds that for the data indicated by open squares. Slope and intercept of the lines are given by Eqs. 5.1 and 5.2, respectively.

Effects of Changes in Filament Growth

We now consider what happens if the conditions that influence filament nucleation and growth are varied. Let us again consider the network to be cross-linked by tetrafunctional junctions. The situation is considerably more

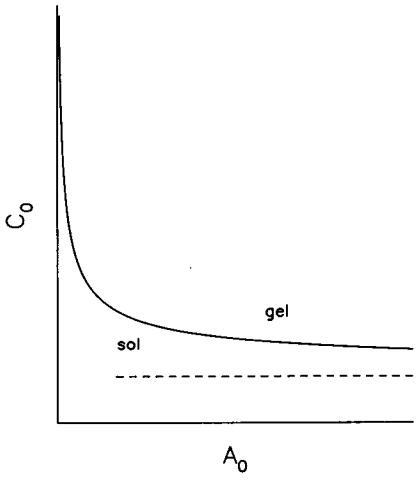

FIGURE 7 Schematic diagram of the 'phase plane' giving the relationship between C_o and A_o necessary for gelation to occur. The boundary between the sol and gel phases is defined by the line $A_o \sim (C_o - K^D)^{-\beta}$, where β here was taken to be 2 (see discussion after Eq. 5.2).

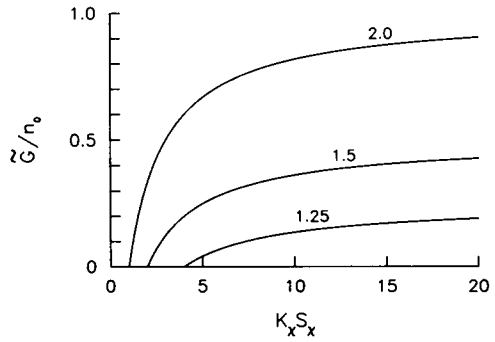

FIGURE 8 The reduced shear modulus $\tilde{G} = G/(\Phi k_\beta V_o^{-1}T)$ plotted as $\tilde{G}/n_o$, shown as a function of the product K_xS_x (see Eq. 3.6). Numbers above curves correspond to different values of A_o/n_o. For a given density of chains (i.e., fixed S_x), the critical value of the binding constant K_x^*, below which gelation does not occur, is given as $K_x^* = [S_x(A_o/n_o - 1)]^{-1}$.

complicated than when chain lengths are fixed. Suppose we vary K^D, which influences the length of the chains (cf. Eq. 4.8). Again, when assuming that $S_x \sim(\Delta C)^\beta \equiv \gamma(\Delta C)^\beta$, we find from Eqs. 3.5, 3.6, 4.6, and 4.7 that $\partial G/\partial K^D$ is given as

$$\frac{1}{\Phi V_o^{-1}k_BT}\frac{\partial G}{\partial K^D} = \frac{\partial A}{\partial K^D} = \frac{A_oK_x}{(1 + K_xS_x)^2}\frac{\partial S_x}{\partial K^D}$$

$$= \frac{-\beta\gamma A_oK_x}{(1 + K_xS_x)^2}(\Delta C)^{\beta-1}, \quad \text{if } \bar{K}_e^D \equiv \frac{k_e^-}{k_e^+e_o} \neq 0 \tag{5.3a}$$

$$= \frac{-\beta\gamma A_oK_x}{(1 + K_xS_x)^2}(\Delta C)^{\beta-1}\left[(1 - e^{-n_ok^+/k_e^+e_o}) + \frac{(C_o - K^D)n_ok^+}{K^Dk_e^+e_o}e^{-n_ok^+/k_e^+e_o}\right], \quad \text{if } \bar{K}_e^D = 0. \tag{5.3b}$$

Eq. 5.3 signifies that, regardless of the values of the rate constants for chain termination, the shear modulus decreases if the average chain length decreases (all other factors being constant). This result is not unexpected, and is characteristic of almost all theories of network elasticity. However, the analytic expressions for the dependence of G on K^D are specific to this model.

A somewhat more surprising result arises when the number of nucleation sites is changed (as might occur in vivo by ligand binding to appropriate receptors on a cell surface). If the capping reactions are reversible, Eqs. 3.5 and 4.6 show that the correlation between G and n_o is negative, namely,

$$\frac{\partial G}{\partial n_o} = -\Phi V_o^{-1}k_BT, \quad \text{if } (\bar{K}_e^D \neq 0) \tag{5.4a}$$

We interpret this to mean that although the number of primary chains increases as n_o increases, their average length decreases and the elastic rigidity consequently also decreases. If, however, the capping events are irreversible, $\partial G/\partial n_o$ is given as shown in Eq. 5.4b:

$$\frac{\partial G}{\partial n_o} = \Phi V_o^{-1}k_BT\left[(C_o - K^D)\left(\frac{k^+}{k_e^+e_o}\right) \cdot \frac{\beta\gamma A_oK_x(\Delta C)^{\beta-1}}{(1 + K_xS_x)^2}e^{-n_ok^+/k_e^+e_o} - 1\right], \quad \text{if } (\bar{K}_e^D = 0). \tag{5.4b}$$

In this case it appears that G can either decrease or increase as n_o varies, depending on the values of other parameters. This complex dependence reflects the fact that the total amount of polymer incorporated into irreversibly capped chains is a sensitive function of n_o. Lastly, if the amount of capping protein is varied, one obtains the relationships

$$\frac{1}{\Phi V_o^{-1}k_BT}\frac{\partial G}{\partial e_o} = 0, \quad \text{if } (\bar{K}_e^D \neq 0) \tag{5.5a}$$

$$= \frac{-\beta\gamma A_oK_x(\Delta C)^{\beta-1}(C_o - K^D)n_ok^+}{(1 + K_xS_x)^2k_e^+e_o^2} \cdot e^{-n_ok^+/k_e^+e_o}, \quad \text{if } (\bar{K}_e^D = 0). \tag{5.5b}$$

VI. COMPETITIVE ACTION OF ACTIN-ASSOCIATED PROTEINS

One of the goals of these investigations is to develop procedures for calculating elasticity phase plane contours appropriate to biophysical modeling of cell contractility (9, 10). Various actin-associated proteins are strongly influenced by local Ca^{2+} concentrations (4, 5, 7, 8). In particular, the activity of fragmenting proteins, which bind to and cut actin chains, is enhanced by Ca^{2+}. Thus, if the Ca^{2+} concentration in the native cytoplasm of motile cells were to increase, there would be a tendency for the elastic modulus to decrease. However, the assembly of myosin within nonmotile cells also is known to depend on Ca^{2+}, by a somewhat complicated mechanism. (Ca^{2+} stimulates the activity of a protein kinase that phosphorylates myosin light chains, such activation being necessary before bipolar myosin filament assembly can occur [1].) Because bipolar myosin filaments will cross-link actin strands, the effect of increased Ca^{2+} in this instance may be to increase elastic rigidity.

When the Ca^{2+} concentration is sufficiently high, capping proteins will fragment actin chains (36). Similar Ca^{2+} ion dependences are known to occur for various α-actinins. (Some, e.g., α-actinin from *Dictyosteleum discoideum*, cross-link actin at low Ca^{2+} and solate actin filaments at high Ca^{2+} [21].) A simple model can be invoked to examine this process. Suppose we consider that an "average chain" of length $r_o = \langle r \rangle$ is subjected to random scissions. If the probability of binding to a site on a chain is proportional to the number of structural units in the chain, then a mass action kinetic equation for scission is

$$\frac{dS^*}{dt} = k_{sc}^+er - k_{sc}^-S^*, \tag{6.1}$$

where S^* is the number of sites at which cutting (and capping) has occurred, e is the concentration of free capping protein, and k_{sc}^+ and k_{sc}^- are rate constants which depend on the Ca^{2+} concentration. Here, r signifies the average number of unbound sites, i.e., $r = r_o - 1 - S^*$. If we assume that the capping protein is in excess or weakly bound, it follows that $e \approx e_o$ and that Eq. 6.1 may be rewritten as

$$\frac{dS^*}{dt} \approx k_{sc}^+ e_o(r_o - 1) - (k_{sc}^- + k_{sc}^+ e_o)S^*. \quad (6.2)$$

If the chains anneal after the dissociation of capping protein (e.g., by hydrogen bounded associations), we construe that, at equilibrium, the number of cuts per average chain $S^*(\infty)$ is given as

$$S^*(\infty) = K_{sc}^{\wedge}(r_o - 1)/(1 + K_{sc}^{\wedge}), \quad (6.3)$$

where $K_{sc}^{\wedge} = k_{sc}^+ \cdot e_o/k_{sc}^-$. Thus, after fragmentation, the number of chains in the assembly can be expressed as

$$n = n_o\left[1 + \frac{K_{sc}^{\wedge}(r_o - 1)}{1 + K_{sc}^{\wedge}}\right] = n_o\left(\frac{1 + K_{sc}^{\wedge} \cdot r_o}{1 + K_{sc}^{\wedge}}\right), \quad (6.4)$$

where n_o signifies the number of primary chains existing in the network before fragmentation occurs. As expected, the number of chains increases, and the average chain length concomitantly decreases.

From Eq. 3.4, for example, it can be seen how the increase in n arising from fragmentation would lead to a decrease in rigidity. It also is apparent from Eq. 3.4 that the assembly of myosin cross-bridges effected by Ca^{2+} tends to increase the elastic modulus. Thus, one can anticipate that stress–strain contours for cytoplasmic extracts which contain both scission proteins and an apparatus for myosin assembly will have features such as those shown in Fig. 9.

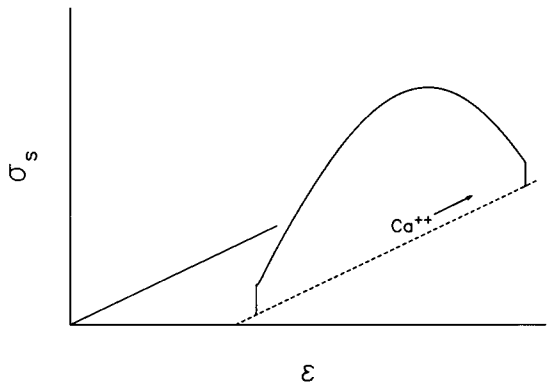

FIGURE 9 Stress profile σ at a given value of strain ϵ. Schematic diagram of the competing effects of Ca^{2+} on network elasticity. For example, Ca^{2+} potentiates the formation of bipolar myosin aggregates that can cross-link actin filaments and thereby increase the elastic modulus. However, at high concentrations, Ca^{2+} increases the activity of scission proteins that weaken the lattice by fragmenting network chains. Certain α-actinins also demonstrate similar Ca^{2+}-dependent cross-linking and solation properties, even in the absence of other actin-associated proteins (21, 22). This figure illustrates how one could derive the phenomenological stress–strain relationships proposed in references 10 and 11.

VII. DISCUSSION AND FURTHER REMARKS

Understanding the physics of cytoplasmic reorganization, along with incumbent cell shape change, is a problem of enormous difficulty (10, 11, 46). Only a very limited aspect of that problem has been addressed in the present work, namely, how the macroscopic parameters that determine the elastic mechanical behavior of the cytogel depend on various attributes of the underlying cytomatrix. The simplest of kinetic schemes have been utilized to describe cytomatix formation, as here we have been interested primarily in establishing calculational procedures and have eschewed any attempts at exact enumeration.

When elastic properties of cytoplasmic gels are considered, one principally is interested in the shear modulus, G, and the changes in that parameter engendered, for example, by changes in the degree of cross-linking of network chains. We have examined, in particular, the relationships between G and the rate constants for molecular associations. Those constants, and similar parameters, may depend on such factors as local pH or Ca^{2+} ion concentration. Given appropriate quantitative data, our results easily could be modified to take such dependences into account. In principle, differences in binding sites along an actin chain (47) also could be accommodated.

We again emphasize that entanglements and various other features of real polymer lattices that affect elastic response have been neglected. In addition to affecting the elastic storage modulus, entanglements and elastically inactive strands ("dangling ends") strongly influence the viscous (i.e., dissipative) parameters of polymer gels. Depending on the time scale of the phenomenon under consideration, such attributes of real lattices can be responsible for a major portion of the stress relaxation and hysteretic behavior of a viscoelastic material.

Also, the assumption that chains are Gaussian probably needs to be modified to obtain a truly quantitative theory of cytoplasmic elasticity; actin filaments, like many other biopolymers, are quite stiff and therefore have long "persistence lengths" (48, 49). Indeed, there is some evidence that actin filaments, in solution, behave as stiff rods (50). In such case entropic contributions to the elastic free energy might have to be augmented by intramolecular energy terms, as characterized by the bending modulus of the rods. Moreover, it should be noted that we implicitly have considered lattice distortions to be small, so that elastic response can be described by Hooke's law ("linear elasticity"). Networks here are assumed to be spatially isotropic, and spatial heterogeneities in local free monomer concentration, which might occur during polymerization

and therefore could affect gel points and gelation rates, have been ignored. These and several similarly difficult aspects of gelation theory currently are being investigated by Monte Carlo computer simulations and renormalization group theory (31, 51).

Another complex phenomenon that has not been examined in the present investigation is the stress relaxation that might result from transient bonding. The annealing (breaking and reforming) of chemical bonds, e.g., monomer–monomer bonding within filaments or cross-linking between strands, might lead to a decrease in mechanical tension that could affect cell shape transformations in important ways (9–14, 46). The relevant molecular parameter is the imaginary part of the shear modulus (often referred to as the loss modulus G [52]), which in certain cases may be characterized in terms of the internal, or solid, viscosity. Theories of stress relaxation for transiently bonded networks are difficult to elaborate and consequently are less developed than for the storage modulus G (see reference 47 for a recent review). It is clear that, at sufficiently high shear rates, stress relaxation will be minimal. Even simple liquids appear to be elastic when subjected to high-frequency mechanical disturbances. Several investigators tend to emphasize the transient nature of the lattice in their analyses of cell motility (11, 12, 53). The exact manner in which network elasticity influences cell motion yet is uncertain, and the fact that the present paper specifically focuses on the elastic storage modulus should not be construed as indicating support for any particular theoretical viewpoint.

Finally, it should be noted that we have considered, explicitly, only responses that involve concurrent displacements of cytomatrix and surrounding solvent, rather than of the polymer matrix alone. However, in some theories of motility the mechanical response of the lattice, by itself, is of central concern (10, 11). In this instance the compressibility modulus of the matrix will be an important parameter but, because the compressibility and shear moduli of the lattice are of the same order of magnitude and are proportional to one another (54, 55), the preceding analysis still pertains. Moreover, in many instances the macroscopic shear modulus of a dilute cross-linked gel is almost identical in magnitude to the shear modulus of the lattice without giving consideration to the fluid phase. Of course, when describing cytoplasmic streaming and other cell phenomena that involve fluid movements, one needs to consider the fact that shear rates might be limited by viscous drag between the fluid and the network.

Despite inherent difficulties in analyzing the properties of complex cytoskeletal networks, important insights into the elastic behavior of such systems can be obtained from relatively simple models. Considering the importance of the many cellular functions that depend on the mechanical transformation of cytoplasm, further work in this area seems to be warranted.

APPENDIX

Derivation of Equation 4.5

Eq. 4.4a can be rewritten as

$$dN/dt = -k_e^+(N - N^+)(N - N^-), \tag{A1}$$

$N^\pm$ being defined by

$$N^\pm = -\tfrac{1}{2}(e_o - n_o - K_e^D) \pm \tfrac{1}{2}[(e_o - n_o - K_e^D)^2 + 4K_e^D e_o]^{1/2}, \tag{A2}$$

where $K_e^D \equiv k_e^-/k_e^+$. When Eq. A1 is rewritten as

$$\frac{1}{(N^+ - N^-)}\left(\frac{1}{N - N^+} - \frac{1}{N - N^-}\right)dN = -k_e^+\,dt$$

and integrated subject to the initial condition $N(0) = n_o$, simple algebraic manipulations yield

$$N(t) = \frac{N^+(n_o - N^-)e^{k_e^+N^+t} - N^-(n_o - N^+)e^{k_e^+N^-t}}{(n_o - N^-)e^{k_e^+N^+t} - (n_o - N^+)e^{k_e^+N^-t}}. \tag{A3}$$

Upon noting that the expression in Eq. A3 can be rewritten as

$$N(t) = \frac{1}{k_e^+}\frac{d}{dt}\ln[(n_o - N^-)e^{k_e^+N^+t} - (n_o - N^+)e^{k_e^+N^-t}], \tag{A4}$$

we then find that the integral appearing in Eq. 4.2 can be evaluated as

$$e^{-k^+\int_0^t N(s)ds} = \left(\frac{(n_o - N^-)e^{k_e^+N^+t} - (n_o - N^+)e^{k_e^+N^-t}}{N^+ - N^-}\right)^{-k^+/k_e^+}. \tag{A5}$$

Thus, by Eq. 4.2.,

$$\Delta C = C_o - C_1(t) = (C_o - K^D) \cdot \left\{1 - \left[\frac{(n_o - N^-)e^{k_e^+N^+t} - (n_o - N^+)e^{k_e^+N^-t}}{N^+ - N^-}\right]^{-k^+/k_e^+}\right\}. \tag{A6}$$

When an assumption is made that e is approximately constant, i.e., that $n_o/e_o \ll 1$, the modified kinetic equation, Eq. 4.4b, ensues. Solution of that equation is similar to the procedure encompassed in Eqs. A1–A6. The limiting behavior, given in Eqs. 4.6 and 4.7, also is a property of Eq. A6: if $k_e^- = 0$, it then follows that $k_e^D = 0$, $N^+ = 0$, $N^- = n_o - e_o$, so that

$$\Delta C(t \to \infty) = (C_o - K^D)\left[1 - \left(\frac{e_o}{e_o - n_o}\right)^{-k^+/k_e^+}\right] \tag{A7}$$

$$\approx (C_o - K^D)(1 - e^{-k^+n_o/k_e^+e_o}). \tag{A8}$$

Eq. A8 follows from Eq. A7 when $n_o \ll e_o$, and is identical to the result given in Eq. 4.7.

Received for publication 26 May 1987 and in final form 23 October 1987.

REFERENCES

1. Alberts, B., D. Bray, J. Lewis, M. Raff, K. Roberts, and J. D. Watson. 1983. The Molecular Biology of the Cell. Garland Press, New York.
2. Porter, K., editor. 1984. The cytoplasmic matrix and the integration of cellular function. *J. Cell Biol.* 99(1, pt. 2):3s–248s.

3. Condeelis, J. S., and D. L. Taylor. 1977. The contractile basis of amoeboid movements. V. The control of gelation, solation and contraction in extracts from dictyostelium discoideum. *J. Cell Biol.* 74:901–927.
4. Pollard, T. D., and J. R. Cooper. 1986. Actin and actin-binding proteins. A critical evaluation of mechanisms and actions. *Annu. Rev. Biochem.* 55:987–1035.
5. Stossel, T. P., C. Chaponnier, R. Ezzell, J. H. Hartwig, P. A. Janmey, D. J. Kwiatkowski, S. E. Lind, D. B. Smith, F. S. Southwick, H. L. Yin, and K. S. Zaner. 1985. Nonmuscle actin-binding proteins. *Annu. Rev. Cell Biol.* 1:353–402.
6. Allen, R. D. 1985. New observations on cell architecture and dynamics by video-enhanced contrast optical microscopy. *Annu. Rev. Biophys. Biophys. Chem.* 14:265–290.
7. Weeds, A. 1982. Actin-binding proteins: regulators of cell architecture and motility. *Nature (Lond.).* 296:811–816.
8. Korn, E. D. 1982. Actin polymerization and its regulation by proteins from nonmuscle cells. *Physiol. Rev.* 62:672–737.
9. Odell, G. M. 1984. A mathematically modelled cytogel cortex exhibits periodic Ca^{++}-modulated contraction cycles seen in *Physarum* shuttle streaming. *J. Embryol. Exp. Morphol.* 83(Suppl.):261–287.
10. Oster, G. F., and G. M. Odell. 1984. Mechanics of cytogels. I. Oscillations in *Physarum*. *Cell Motil.* 4:469–503.
11. Dembo, M., and F. Harlow. 1986. Cell motion, contractile networks, and the physics of interpenetrating reactive flow. *Biophys. J.* 50:109–121.
12. Dembo, M. 1986. The mechanics of motility in dissociated cytoplasm. *Biophys. J.* 50:1165–1183.
13. Oster, G. F., J. D. Murray, and G. M. Odell. 1985. The formation of microvilli. *In* Molecular Determinants of Animal Form. G. M. Edelman, editor. Alan R. Liss, New York. 365–384.
14. Oster, G. F. 1984. On the crawling of cells. *J. Embryol. Exp. Morphol.* 83(Suppl.):329–364.
15. Schmid-Schonbein, G. W., and R. Skalak. 1984. Continuum mechanical model of leukocytes during protopod formation. *J. Biomech. Eng.* 106:10–18.
16. MacLean-Fletcher, S. D., and T. D. Pollard. 1980. Viscometric analysis of the gelation of *Acanthamoeba* extracts and purification of two gelation factors. *J. Cell Biol.* 85:414–428.
17. Zaner, K. S., and T. P. Stossel. 1982. Some perspectives on the viscosity of actin filaments. *J. Cell Biol.* 93:987–991.
18. Zaner, K. S. 1986. The effect of the 540-kilodalton actin cross-linking protein, actin-binding protein, on the mechanical properties of F-actin. *J. Biol. Chem.* 261:7615–7620.
19. Pearson, D. S., and W. W. Graessley. 1978. The structure of rubber networks with multifunctional junctions. *Macromolecules.* 11:528–533.
20. Flory, P. J. 1953. Principles of Polymer Chemistry. Cornell University Press, Ithaca, NY.
21. Simon, J. R., R. Furukawa, D. L. Taylor, and B. Ware. 1987. The dynamic interaction of *D. discoideum* α-actinin with F-actin. *Biophys. J.* 51:392a.
22. Sato, M., W. H. Schwarz, and T. D. Pollard. Dependence of the mechanical properties of actin/α-actinin gels on deformation rate. *Nature (Lond.).* 325:828–830.
23. Hartwig, J. H., and T. P. Stossel. 1981. The structure of actin-binding protein molecules in solution and interacting with actin filaments. *J. Mol. Biol.* 145:563–581.
24. Niederman, R., P. C. Amrein, and J. Hartwig. 1983. Three-dimensional structure of actin filaments and of an actin gel made with actin-binding protein. *J. Cell Biol.* 96:1400–1413.
25. Hartwig, J. H., J. Tyler, and T. P. Stossel. 1980. Actin-binding protein promotes and bipolar and perpendicular branching of actin filaments. *J. Cell Biol.* 87:841–848.
26. Graessley, W. W. 1975. Elasticity and chain dimensions in Gaussian networks. *Macromolecules.* 8:865–868.
27. Flory, P. J. 1977. Theory of elasticity of polymer networks. The effect of local constraints on junctions. *J. Chem. Phys.* 66:5720–5729.
28. Scanlan, J. 1960. The effect of network flaws on the elastic properties of vulcanizates. *J. Polym. Sci.* 43:501–508.
29. Case, L. C. 1960. Branching in polymers. I. Network defects. *J. Polym. Sci.* 45:397–404.
30. Nossal, R. 1985. Network formation in polyacrylamide gels. *Macromolecules.* 18:49–54.
31. Bansil, R., H. J. Herrmann, and D. Stauffer. 1985. Kinetic percolation with mobile monomers and solvents as a model for gelation. *J. Polym. Sci. Polym. Symp.* 73:175–180.
32. de Gennes, P.-G. 1979. Scaling Concepts in Polymer Physics. Cornell University Press, Ithaca, NY.
33. Nossal, R. 1987. In vitro polymerization of complex cytoplasmic gels. *In* Reversible Polymeric Gels and Related Systems. Paul S. Russo, editor. American Chemical Society, Washington, DC.
34. Isenburg, G., U. Aebi, and T. D. Pollard. 1980. An actin-binding protein from *Acanthamoeba* regulates actin filament polymerization and interactions. *Nature (Lond.).* 288:455–459.
35. Isenburg, G., R. Ohnheiser, and H. Maruta. 1983. 'Cap 90', a 90-KDa Ca-dependent F-actin-capping protein from vertebrate brain. *FEBS (Fed. Eur. Biochem. Soc.) Lett.* 163:225–229.
36. Yin, H. L., and T. P. Stossel. 1979. Control of cytoplasmic actin gel-sol transformation by gelsolin, a calcium-dependent regulatory protein. *Nature (Lond.).* 281:583–586.
37. Petrucci, T. C., C. Thomas, and D. Bray. 1983. Isolation of a Ca-dependent actin-fragmenting protein from brain, spinal cord, and cultured neurons. *J. Neurochem.* 40:1507–1516.
38. Lin, D. C., and S. Lin. 1979. Actin polymerization induced by a motility-related high-affinity cytochalasin binding complex from human erythrocyte membrane. *Proc. Natl. Acad. Sci. USA.* 76:2345–2349.
39. Geiger, B., Z. Avnur, G. Rinnerthaler, H. Hinssen, and J. V. Small. 1984. Microfilament-organizing centers in areas of cell contact: cytoskeletal interactions during cell attachment and locomotion. *J. Cell Biol.* 99(1, pt. 2):83s–91s.
40. Mangeat, P., and K. Burridge. 1984. Actin-membrane interaction in fibroblasts: what proteins are involved in this association? *J. Cell Biol.* 99(1, pt. 2):95s–103s.
41. Oosawa, F., and S. Asakura. 1975. Thermodynamics of the Polymerization of Protein. Academic Press, Inc., New York.
42. Brown, S. S., and J. A. Spudich. 1979. Nucleation of polar actin filament assembly by a positively charged surface. *J. Cell Biol.* 80:499–504.
43. Wegner, A. 1976. Head to tail polymerization of actin. *J. Mol. Biol.* 108:139–150.
44. Pantaloni, D., T. L. Hill, M.-F. Carlier, and E. D. Korn. 1985. A new model for actin polymerization and the kinetic effects of ATP hydrolysis. *Proc. Natl. Acad. Sci. USA.* 82:7207–7211.
45. Hill, T. L. 1986. Theoretical study of a model for the ATP cap at the end of an actin filament. *Biophys. J.* 49:981–986.
46. Oster, G. F., and A. S. Perelson. 1985. Cell spreading and motility: a model lamellipod. *J. Math. Biol.* 21:383–388.
47. Klonowski, W., and I. R. Epstein. 1987. Kinetics of actin-myosin binding. II. Two-variable model and actin gelation. *Biophys. J.* 51:249–253.
48. Klonowski, W. 1985. Probabilistic-topological representation for crosslink, entanglement, or contact networks in (bio)polymer systems. *J. Appl. Physiol.* 58:2883–2892.
49. Edwards, S. F. 1986. The theory of macromolecular networks. *Biorheology.* 23:589–603.
50. Ito, T., K. S. Zaner, and T. P. Stossel. 1987. Nonideality of volume flows and phase transitions of F-actin solutions in response to osmotic stress. *Biophys. J.* 51:745–754.
51. Family, F., and D. P. Landau, editors. 1984. Kinetics of aggregation and gelation. Elsevier North-Holland, Amsterdam.

52. Ferry, J. D. 1980. Viscoelastic properties of polymers. 3rd ed. John Wiley & Sons, Inc., New York.
53. Buxbaum, R. E., T. Dennerll, S. Weiss, and S. R. Heidemann. 1987. F-actin and microtubule suspensions as indeterminate fluids. *Science (Wash. DC).* 235:1511–1514.
54. Landau, L. D., and E. M. Lifshitz. 1959. Theory of Elasticity. Addison-Wesley, Reading, MA.
55. Tanaka, T., L. O. Hocker, and G. B. Benedek. 1973. Spectrum of light scattered from a viscoelastic gel. *J. Chem. Phys.* 59:5151–5159.